

Investigation of Post Annealing Effect on the PZT Thin Films

Sujin Choi¹, Juyun Park¹, Sung-Wi Koh², and Yong-Cheol Kang^{1*}

Abstract

The PZT thin films were deposited on Si(100) substrate using RF magnetron sputtering method. And the PZT thin films were post annealed at various temperatures to form perovskite phase. To analyze PZT thin films, surface profiler, XRD, XPS, CA, and SFE were used. The thickness increased from 536.5 to 833.2 nm as post annealing temperature increased. The perovskite PZT was observed from PZT-823 and pyrochlore PZT, ZrO₂, TiO₂, and perovskite PbZrO₃ were observed. From the XPS, the atomic percentages of Pb, Zr, Ti, and O were calculated and the portion of Pb increased to PZT-823 and decreased to PZT-923 and then increased to PZT-1023. Also, the CA and SFE was effected on post annealing temperature and as a function of atomic percentage of Pb, the CA and SFE was transformed.

Keywords: Thin Film, X-ray Diffraction, Lead Zirconate Titanate

1. Introduction

Lead zirconate titanate (Pb(Zr_{1-x}Ti_x)O₃, PZT) has ferroelectric, piezoelectric, and dielectric properties. Due to that properties, PZT is important and commonly used material in the fields of microsystems and microelectronics^[1,2]. The PZT thin films have been regarded widely as ferroelectric random access memories, non-volatile memory devices, and dynamic access memories because of their stability as operating in devices and their remarkable ferroelectric properties^[3-6].

Previously reported, Bose *et al.* fabricated PZT thin films with radio frequency (RF) sputtering and the substrate was heated during sputtering at 673 K. The obtained PZT thin films were post annealed at 823 K for 3 min and 5 min respectively. The PZT thin film post annealed for 3 min shown perovskite and pyrochlore phase. And 5 min post annealed PZT thin film was pyrochlore phase^[7]. And Bhaskar *et al.* obtained PZT thin films using sol-gel method and post annealing with microwave from 673 to 973 K. From 723 to 823 K, only perovskite phase was observed, however, with annealing temperature increased per-

ovskite phased decreased^[8].

In this research, the PZT thin films were fabricated with reactive RF magnetron co-sputtering method using metallic Pb, Zr, and Ti targets. And the obtained PZT thin films were post annealed at various temperature to fabricate perovskite PZT thin films. The thickness of annealed PZT thin films at various temperatures was measured with a surface profiler. The crystallinity of the PZT thin films were monitored with X-ray diffraction (XRD) and the stoichiometry of PZT thin films fabricated at various post annealing temperatures was investigated with X-ray photoelectron spectroscopy (XPS).

2. Experimental Section

The PZT thin films were fabricated by reactive RF magnetron co-sputtering method on n-type Si(100) used as substrate. The n-type Si(100) substrate was cleaned with acetone prior to install in co-sputtering chamber. During deposition, the n-type Si(100) substrate was heated at 573 K and the substrate holder was rotated at 5 rpm to be deposited uniformly. The co-sputtering chamber was evacuated about 2.6×10^{-6} Torr with a rotary vane pump (RP) and a turbo molecular pump (TMP). As PZT thin films were deposited, the working pressure was kept about 4.5×10^{-2} Torr. The PZT thin films were deposited using metal lead (Pb), zirconium (Zr), and titanium (Ti) targets for co-sputtering. And RF power was applied independently at each target such as

¹Department of Chemistry, Pukyong National University, 45, Yongso-ro, Nam-Gu, Busan, 608-737, Korea

²Department of Mechanical System Engineering, Pukyong National University, Busan 608-739, Korea

*Corresponding author : yckang@pknu.ac.kr

(Received: November 8, 2015, Revised: December 16, 2015

Accepted: December 25, 2015)

30, 200, and 250 W for Pb, Zr, and Ti targets, respectively. The pre-sputtering was performed for 10 min to stabilize the plasma and to remove the contaminants on the metal targets. And then co-sputtering was conducted for 10 min. The obtained PZT thin film was post annealed at 823, 923, and 1023 K in ambient atmosphere for 2 h. Here on after, PZT-X was notated that the PZT films post annealed at X Kelvin. The post annealed PZT thin film at 823 K was denote as PZT-823. In order to measure the thickness of the deposited PZT thin films, a surface profiler (Alpha-Step 500, Tencor, USA) was used and the edge of substrate was masked with Kapton® tape before installing in the co-sputtering chamber. The crystallinity of PZT thin films was investigated with X-ray diffraction (XRD, X-pert pro, Netherlands). Surface free energy (SFE) and hydrophilicity were evaluated with the contact angles (CA) of the liquids on PZT thin films. The contact angles were tested and measured with distilled water (DW) and ethylene glycol (EG) by means of home-made contact angle measurement system. The chemical environment and oxidation states of each atom on PZT thin films were investigated with X-ray photoelectron spectroscopy (XPS, ESCALab MKII, VG, UK) with using Mg K α X-ray source (1253.6 eV). The XPS analysis was conducted in an ultrahigh vacuum (UHV) chamber, the base pressure of the UHV chamber was kept below 3.0×10^{-10} Torr by means of a RP, a TMP, two Ti-sublimation pumps, and two ion pumps. The XPS spectra were obtained with a concentric hemispherical analyzer in constant analyzer energy mode. Deconvolution process was performed with XPSPEAK41 software (ver 4.1) in the 30% of Gaussian/Lorentzian ratio to determine the atomic ratios and oxidation states of Pb, Zr, Ti, and O.

3. Results and Discussion

The thickness of post-annealed PZT thin films was measured with surface profiler and the results are shown in Fig. 1. The thickness increased gradually as the post annealing temperature increased. The thickness increased from 536.5 to 833.2 nm for PZT-823 and PZT-1023, respectively. The roughness increased as post-annealing was performed. From XRD pattern shown in Fig. 2, as annealing temperature increased, the PZT thin films showed multi-phase. Due to the space

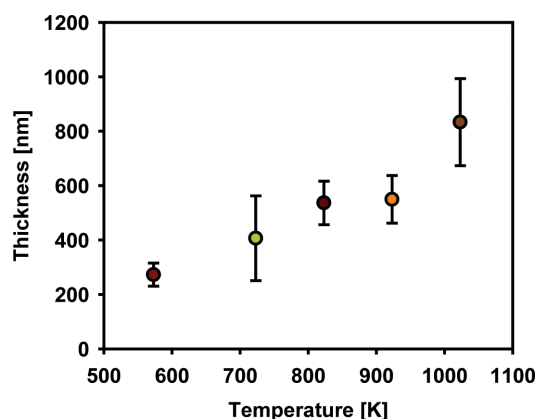


Fig. 1. The thickness of PZT thin films.

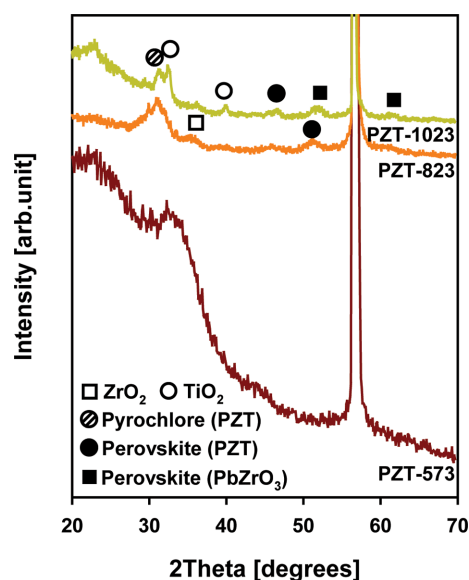


Fig. 2. XRD patterns of post annealed PZT films.

between various structures, the thickness of the thin film with multi-phase increased as post annealing temperature increased.

The crystallinity of annealed PZT thin films shown and the phase transition was observed with respect to post annealing temperature as shown in Fig. 2. The phases were transformed from amorphous to pyrochlore and perovskite phases of PZT. The diffraction angles of 30.9, 31.3, 46.6, and 50.6° [JCPDS 33-0784, 73-2022] were assigned to perovskite phase of PZT. The 51.9 and 60.3° were presented perovskite of PbZrO₃. And 34.5 and 40.0° were assigned to tetragonal ZrO₂ [JCPDS

88-1007] and tetragonal TiO_2 [#JCPDS 88-1174], respectively. At low diffraction angle, about from 29 to 33°, a broad peak was observed so, the broad peak was performed deconvolution process to assign the hidden peaks exactly.

The deconvoluted from 29° to 33° XRD patterns are shown in Fig. 3. The peaks 30.2 and 31.3° were assigned to perovskite of PZT and 30.4, 31.8, and 32.3° were assigned for PbZrO_3 [#JCPDS 88-0270, 88-0271]. And the diffraction angles of 30.0 and 29.2° presented PZT pyrochlore [#JCPDS 26-0142] and Pb_2O_3 [#JCPDS 73-1284, 76-1791]. In Fig. 3, the perovskite phases of PZT and PbZrO_3 increased and pyrochlore and Pb_2O_3 phases decreased. Hiremath *et al.* reported the formation of PbZrO_3 and PbTiO_3 were intermediate compounds to form PZT formation. To form PZT compound, the PbTiO_3 reacts with PbO , PbTi_3O_7 and PbZrO_3 and then the PbZrO_3 reacts with PbTiO_3 .^[9] And Thomas *et al.* reported that existence of enough Pb could form PbO and the PbO was intermediate to form PZT formation^[10]. Due to enough Pb_2O_3 and PbZrO_3 , the perovskite PZT increased with post annealing temperature increased. Above 1023 K, the perovskite PZT enable to exist in the PZT thin film for the rich PbZrO_3 . In Fig. 2 and 3, as post annealing temperature increased, the phases were transformed from pyrochlore to perovskite. The structure of PZT films was transformed from amorphous through pyrochlore to perovskite as post annealing temperature increased. This result was well correlated with other group's^[11].

To study the composition and chemical environment of PZT thin films, the XPS analysis was performed. For more chemical information from the post annealed PZT thin films, the narrow XPS was conducted and performed deconvolution process. The representative narrow XPS and deconvoluted of Pb 4f and Zr 3d were shown in Fig. 4. In Fig. 4(a), the intensity of Pb 4f increased as post annealed at 823 K and maintained that level with respect to increase of post annealing temperature. Also the shape of the peak was dramatically changed from PZT-573 to PZT-823 and from PZT 923 to PZT-1023 therefore, the PZT-573, 923, and 1023 was deconvoluted representatively. The peaks of Pb 4f were fitted with Pb^0 (136.1±0.1 eV), Pb^{4+} (137.2±0.1 eV), Pb^{2+} in PZT (138.3±0.1 eV), and PbZrO_3 (139.2±0.1 eV)^[12-15]. The Pb^{4+} , dominant Pb^{2+} , and small amount Pb^0 were existed in PZT-573 however in PZT-923, the Pb^{4+} was dominant oxidation state. Due to the high level of Pb^{4+} , the perovskite PZT decreased in PZT-923 from Fig. 3. In PZT-1023, result from the increment of Pb^{2+} the perovskite phase increased. The small level of PbZrO_3 was observed as shown in Fig. 4(a) and the perovskite of PbZrO_3 dramatically increased at Fig. 3.

In the Fig. 4(b), the narrow XPS spectra and deconvoluted XPS spectra were showed. As post annealing temperature increased the peak of Zr 3d was red shifted and the intensity drastically declined. The Zr 3d was deconvoluted with three peaks and assigned to Zr combined with surface or carbon (Zr-C, 180.5±0.1 eV), Zr^{4+} in PZT (181.9±0.1 eV), and ZrO_2 (183.3±0.1 eV)^[16-19]. As post annealing temperature increased, the portion of Zr^{4+} gradually decreased while Zr-C increased steadily though the Zr^{4+} to form the PZT was dominant. And existence of ZrO_2 was confirmed from XPS and XRD

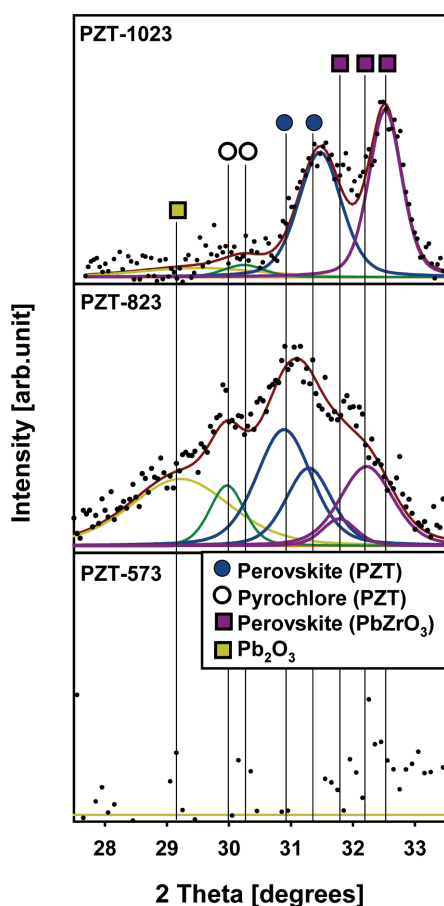


Fig. 3. The deconvoluted XRD.

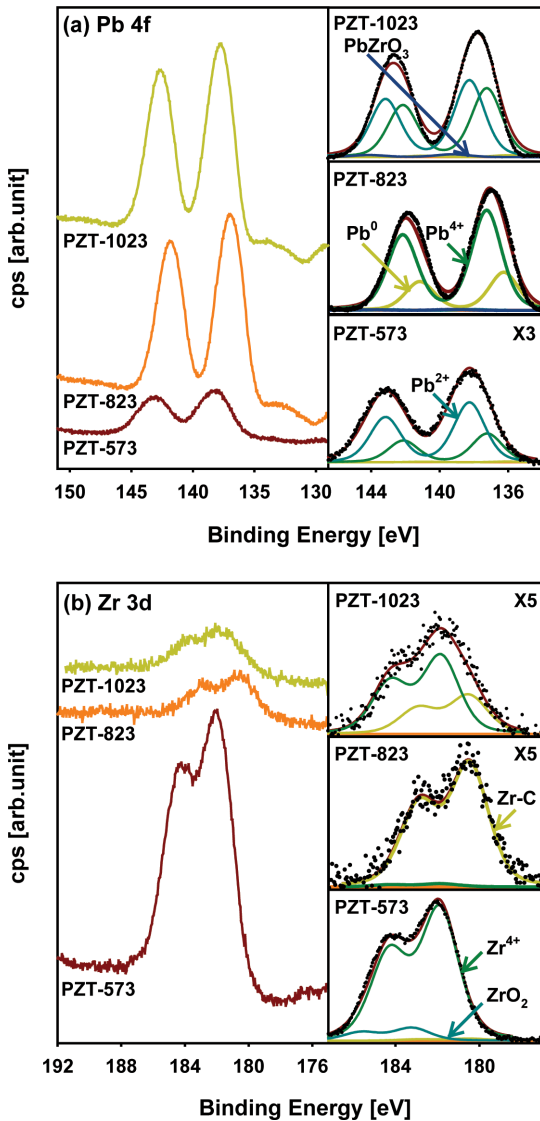


Fig. 4. The representative XPS narrow and deconvoluted spectra of (a) Pb 4f and (b) Zr 3d.

results. Although the dominant oxidation states to form PZT compound was sufficient at PZT-573 the perovskite PZT formation was not observed. Because the intensity of Pb was insufficient compared with Zr and the detail of that Pb and Zr portion was explained in Fig. 5. That XPS results was correspond with other studies that the enough Pb portion was important to form perovskite PZT formation^{9,10}. And the change of intensity about Pb 4f and Zr 3d was explained that the Pb and Zr was migrated, diffused, and/or segregated

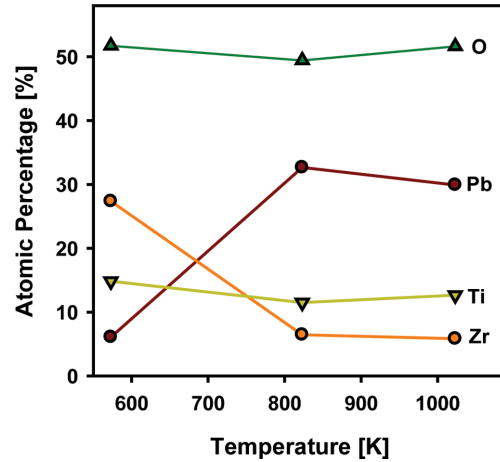


Fig. 5. The atomic percentage of PZT thin films.

from or to bulk. That phenomenon was well agreed with other group's research^{4,20}. Therefore the effect of post annealing, the Pb was diffused or migrated to surface and Zr was diffused or migrated to bulk.

From the deconvoluted XPS, the atomic percentages of post annealed PZT thin films were calculated and that results were showed at Fig. 5. As PZT thin film was post annealed at 823 K, the portion of Pb drastically increased from 6.1 to 32.7% and Zr decreased from 27.4 to 6.4%. And then as post annealing temperature increased, the atomic percentages of Pb and Zr were showed consistent level about 29.7 and 8.3% respectively. The atomic percentages of O and Ti were maintained steady value about 50.9 and 12.2%, respectively. The portion of Pb and Zr was well corresponded with XPS and XRD results. The lack of Pb, the perovskite PZT was not observed at PZT-573 from XRD. From the PZT-823, due to sufficient Pb portion the perovskite phase of PZT and PbZrO₃ were formed.

The CA measurement is a common method to characterize surface of various thin films. At Fig. 6, the CA and SFE of as a function of post annealing temperature of PZT thin films measured using DW and EG were showed. The SFE was calculated using Young's equation²¹. The total SFE is the sum of polar SFE and dispersive SFE. The polar SFE was depended on such as dipole-dipole, dipole-dipole induced, hydrogen bonding, and acid-base interaction. The dispersive SFE was resulted from non-polar interaction between surface and bulk. Originally low CA high total SFE due to the low CA meant strong energy between surface of the mate-

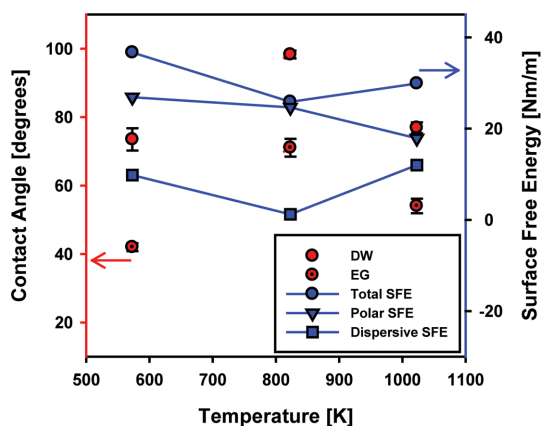


Fig. 6. The contact angle and surface free energy of PZT thin films.

rial and liquid such as DW or EG. In Fig. 6, as post annealing temperature increased CA of EG showed decreasing propensity from PZT-823 to PZT-1023 from 71.1 to 54.0°. While the CA of DW decreased from PZT-823 to PZT-923 and then increased to PZT-1023. The CA measured with DW was well correlated with atomic percentage of Pb. And the low CA means that the surface was not stable. From the sufficient Pb, the perovskite phase PZT could form with Zr, Ti and O. From the Fig. 2 and 3, the perovskite phase of PZT compound showed similar tendency of CA and atomic percentage of Pb. Therefore, due to the enough Pb the perovskite phased was formed and the surface was transformed stable.

4. Conclusion

The PZT thin films were fabricated with RF magnetron sputtering method and post annealed at various temperature. As post annealing temperature increased, the thickness of the PZT thin films increased for various structure. From the XRD, the perovskite phase of PZT and PbZrO_3 was observed and the perovskite phase increased as post annealing temperature increased. And the crystallinity of PZT thin films was transformed from amorphous to perovskite phase. To study about composition and chemical environment of PZT thin films the XPS analysis was constructed. From XPS result, the Pb^{2+} and Zr^{4+} were dominant at PZT-1023 and the peak was shifted to red shift as post annealing temperature increased. The CA and SFE results was well corre-

sponded with atomic percentage of Pb and XRD results. Due to lack of Pb, the surface was unstable and the low CA were showed.

Acknowledgement

This work was supported by Research Grant of Pukyong National University (2015 year : C-D-2015-0718).

References

- [1] C.C. Chang and C.S. Tang, "An integrated pyroelectric infrared sensor with a PZT thin film", *Sensor. Actuat. A-Phys.*, Vol. 65, pp. 171-174, 1998.
- [2] W. Zhu, K. Yao, and Z. Shang, "Novel structured multilayer piezoelectric PZT micro-actuators using screen printing technology", *Ferroelectrics*, Vol. 224, pp. 153-160, 1999.
- [3] F. Chen, R. Schafranek, S. Li, W. B. Wu, and A. Klein, "Energy band alignment between $\text{Pb}(\text{Zr,Ti})\text{O}_3$ and high and low work function conducting oxides from hole to electron injection", *J. Phys. D Appl. Phys.*, Vol. 43, pp. 295301(6pp), 2010.
- [4] A. Bose and M. Sreemany, "Influence of processing conditions on the structure, composition and ferroelectric properties of sputtered PZT thin films on Ti-substrates", *Appl. Surf. Sci.*, Vol. 289, pp. 551-559, 2014.
- [5] M. M. Zhu, Z. H. Du, and J. Ma, "Defect enhanced optic and electro-optic properties of lead zirconate titanate thin films", *AIP Adv.*, Vol. 1, pp. 042144, 2011.
- [6] C. H. Park, M. S. Won, C. S. Lee, W. H. Cha, and Y. G. Son, "Pyroelectric properties and X-ray photoelectron spectroscopic study of R.F. magnetron-sputtering-derived PZT thin films deposited on various interlayers", *J. Electroceram.*, Vol. 17, pp. 619-623, 2006.
- [7] A. Bose, S. Bysakh, M. Mukherjee, A. K. M. Maidul Islam, A. K. Balamurugan, and S. Sen, "Characterization of RF sputter-deposited ultra thin PZT films and its interface with substrate", *Integr. Ferroelectr.*, Vol. 120, pp. 37-48, 2010.
- [8] A. Bhaskar, H. Y. Chang, T. H. Chang, and S. Y. Cheng, "Effect of microwave annealing temperatures on lead zirconate titanate thin films", *Nanotechnology* Vol. 18, pp. 395704(7pp), 2007.
- [9] C. V. R. Vasant Kumar, R. Pascual, and M. Sayer,

- “Crystallization of sputtered lead zirconate titanate films by rapid thermal processing”, *J. Appl. Phys.*, Vol. 71, pp. 864-874, 1992.
- [10] R. Thomas, S. Mochizuki, T. Mihara, and T. Ishida, “Effect of substrate temperature on the crystallization of $\text{Pb}(\text{Zr,Ti})\text{O}_3$ films on Pt/Ti/Si/ substrates prepared by radio frequency magnetron sputtering with a stoichiometric oxide target”, *Mater. Sci. Eng. B-Adv.*, Vol. 95, pp. 36-42, 2002.
- [11] K. G. Brooks, I. M. Reaney, R. Klissurska, Y. Huang, L. Brusill, and N. Setter, “Orientation of rapid thermally annealed lead zirconate titanate thin films on (111) Pt substrates”, *J. Mater. Res.*, Vol. 9, pp. 2540-2553, 1994.
- [12] N. Wakiya, K. Kuroyanagi, Y. Xuan, K. Shinozakim, and N. Mizutani, “An XPS study of the nucleation and growth behavior of an epitaxial $\text{Pb}(\text{Zr,Ti})\text{O}_3/\text{MgO}(110)$ thin film prepared by MOCVD”, *Thin Solid Films*, Vol. 372, pp 156-162, 2000.
- [13] J. Yu, J. C. Yu, B. Cheng, and X. Zhao, “Photocatalytic activity and characterization of the sol-gel derived Pb-doped TiO_2 thin films”, *J. Sol-Gel Sci. Techn.*, Vol. 24, pp. 39-48, 2002.
- [14] J. M. Koo, H. S. Min, W. H. Lee, J. G. Lee, J. Y. Kim, and J. H. Ahn, “Influences of hydrogen damages in ferroelectric thin film capacitors”, *Ferroelectrics*, Vol. 260, pp. 279-284, 2001.
- [15] P. Verardi, F. Craciun, L. Mirengi, M. Dinescu, and V. Sandu, “An XPS and XRD study of physical and chemical homogeneity of $\text{Pb}(\text{Zr,Ti})\text{O}_3$ thin films obtained by pulsed laser deposition”, *Appl. Surf. Sci.*, Vol. 138-139, pp. 552-556, 1999.
- [16] F. Bortolani, A. Campo, J. F. Fernandez, F. Clemens, and F. Rubio-Marcos, “High strain in $(\text{K,Na})\text{NbO}_3$ -based lead-free piezoelectric fibers”, *Chem. Mater.*, Vol. 26, pp. 3838-3848, 2014.
- [17] K. Idczak, M. Skiścim, and L. Markowski, “Comparison of the adsorption of thin zirconium and titanium oxides films on the 6H-SiC(0001) surface”, *Cryst. Res. Technol.*, Vol. 47, pp. 329-332, 2012.
- [18] X. G. Tang, A. L. Ding, and W. G. Luo, “Surface morphology and chemical states of highly oriented PbZrO_3 thin films prepared by a sol-gel process”, *Appl. Surf. Sci.*, Vol. 174, pp. 148-154, 2001.
- [19] A. C. Galca, V. Stancu, M. A. Husanu, C. Dragoi, N. G. Gheorghe, L. Trupina, M. Enculescu, and E. Vasile, “Substrate-target distance dependence of structural and optical properties in case of $\text{Pb}(\text{Zr,Ti})\text{O}_3$ films obtained by pulsed laser deposition”, *Appl. Surf. Sci.*, Vol. 257, pp. 5938-5943, 2011.
- [20] C. H. Park, M. S. Won, Y. H. Oh, and Y. G. Son, “An XPS study and electrical properties of $\text{Pb}_{1.1}\text{Zr}_{0.53}\text{Ti}_{0.47}\text{O}_3/\text{PbO}/\text{Si}$ (MFIS) structures according to the substrate temperature of the PbO buffer layer”, *Appl. Surf. Sci.*, Vol. 252, pp. 1988-1997, 2005.
- [21] A. A. Ogbu, E. Bouquerel, O. Ademosu, S. Moh, E. Crossan, and F. Placido, “An investigation of the surface energy and optical transmittance of copper oxide thin films prepared by reactive magnetron sputtering”, *Acta. Mater.*, Vol. 53, pp 5151-5159, 2005.